

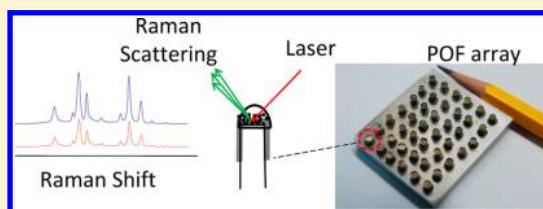
# Sensitive Cylindrical SERS Substrate Array for Rapid Microanalysis of Nucleobases

Panneerselvam Rajapandiyan and Jyisy Yang\*

Department of Chemistry and Center of Nanoscience and Nanotechnology, National Chung-Hsing University, Taichung 402, Taiwan

**S** Supporting Information

**ABSTRACT:** In this work, a cylindrical-substrate array for surface-enhanced Raman scattering (SERS) measurements was developed to enable analysis of nucleobases in a few microliters of liquid. To eliminate uncertainties associated with SERS detection of aqueous samples, a new type of cylindrical SERS substrate was designed to confine the aqueous sample at the tip of the SERS probe. Poly(methyl methacrylate) (PMMA) optical fibers in a series of different diameters were used as the basic substrate. A solution of poly(vinylidene fluoride)/dimethylformamide (PVDF/DMF) was used to coat the tip of each fiber to increase the surface roughness and facilitate adsorption of silver nanoparticles (AgNPs) for enhancing Raman signals. A chemical reduction method was used to form AgNPs in and on the PVDF coating layer. The reagents and reaction conditions were systematically examined with the aim of estimating the optimum parameters. Unlike the spreading of aqueous sample on most SERS substrates, particularly flat ones, the new SERS substrates showed enough hydrophobicity to restrict aqueous sample to the tip area, thus enabling quantitative analysis. The required volume of sample could be as low as 1  $\mu\text{L}$  with no need for a drying step in the procedure. By aligning the cylindrical SERS substrates into a solid holder, an array of cylindrical substrates was produced for mass analysis of aqueous samples. This new substrate improves both reproducibility and sensitivity for detection in aqueous samples. The enhancement factor approaches 7 orders in magnitude with a relative standard error close to 8%. Using the optimized conditions, nucleobases of adenine, cytosine, thymine, and uracil could be detected with limits approaching a few hundreds nanomolar in only a few microliters of solution.



The phenomenon of surface-enhanced Raman scattering (SERS) has been observed for molecules adsorbed on the surfaces of nanosized metals. In general, this behavior is explained by the effects of electromagnetic field and charge-transfer,<sup>1,2</sup> and the commonly observed factors influencing the magnitude of the enhancements include the morphologies and species of metals and the molecule itself.<sup>3–5</sup> To prepare highly sensitive SERS substrates, a wide range of methods have been developed. For instance, SERS substrates can be prepared by electrochemical roughening,<sup>6,7</sup> formation of metal colloids,<sup>8,9</sup> vapor deposition of island films,<sup>10</sup> silver-doped sol–gel films,<sup>11–13</sup> and the silver mirror reaction.<sup>14–17</sup> Among these methods, the silver mirror reaction offers several advantages, including low cost, no need for sophisticated equipment, and no limitation on the base substrate shape. Substrates such as glass,<sup>17</sup> copper foil,<sup>18</sup> silicon, aluminum foil,<sup>19</sup> and celluloses<sup>20–23</sup> with different shapes and sizes have been successfully treated. Also, an enhancement factor of  $10^6$  can be obtained easily. Successful applications of these SERS substrates has been demonstrated to obtain structural information<sup>24,25</sup> and biological information.<sup>26,27</sup> With proper treatment, SERS substrates can be used for trace analysis,<sup>28,29</sup> single molecule detections,<sup>30,31</sup> and SERS nanoimaging.<sup>32–35</sup>

However, several problems are associated with detection of species in aqueous solutions. For example, with nanoparticle-treated SERS substrates, extensive analysis time usually is needed to evaporate the water from aqueous samples. Also, the uncertainty in spreading of aqueous samples on the SERS

substrate causes serious problems with reproducibility. To remove the water, several methods have been reported.<sup>20,22,36</sup> Huang et al.<sup>36</sup> used gentle heat to dry the analyte-doped AgNPs, and an enhancement factor up to  $10^6$  was obtained with a short analysis time. Another approach utilized a colloidal solution of AgNPs mixed with samples and deposited on filter paper to drain the water. The detection limit approached a few hundred nanograms for Raman-sensitive dyes as demonstrated by Tran et al.<sup>20</sup> However, for less Raman-active molecules such as amino acids, an enhancement factor of 30 was obtained by employing the same procedures as demonstrated by Ota et al.<sup>22</sup> Also, the detection procedures usually require drying via heating of the samples, which seriously decrease the SERS enhancement due to surface oxidation of AgNPs.<sup>37</sup>

To solve the problems associated with analysis of aqueous samples, novel cylindrical SERS substrates were developed in this work. These new substrates utilize hydrophobicity of polymeric materials to confine aqueous samples to a small region around the sensor tip. Low-cost poly(methyl methacrylate) (PMMA) optical fiber was employed, and its tip (the cross section of the fiber) was treated with AgNPs to form a SERS active area. By depositing small amount of aqueous samples, the surface tension of water forms an aqueous sample

Received: July 30, 2012

Accepted: November 9, 2012

Published: November 9, 2012

drop at the tip of the cylindrical SERS substrates, which solves the water-spreading problem commonly observed with planar substrates. To increase the roughness of the tip surface and the resulting contact area, a thin layer of poly(vinylidene fluoride) (PVDF) was coated on the tip of the PMMA fiber before deposition of AgNPs. PVDF is hydrophobic and is known to be compatible with PMMA fiber. It has been used frequently as a coating layer for PMMA optical fiber.<sup>38,39</sup> The silver mirror reaction was employed to grow AgNPs on the tip surface, because it is a low cost method suited to irregular and/or roughened surfaces. The procedure used in this work to produce cylindrical SERS substrates is shown schematically in Figure 1. The resulting SERS substrates require only small

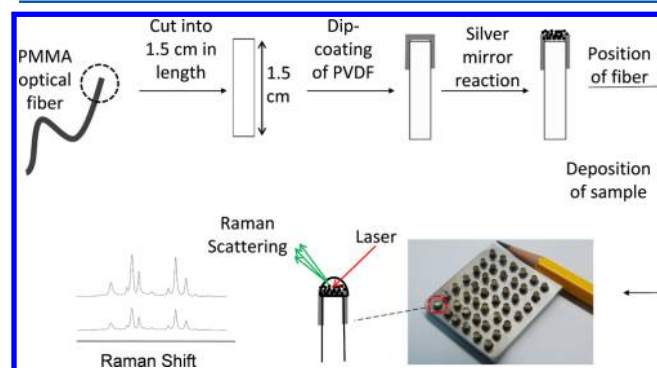


**Figure 1.** Schematic diagram for preparation of cylindrical SERS substrate and SERS substrate array for microanalysis of nucleobases.

sample volumes with no drying for the detection of biological samples. The oxidation of AgNPs associated with the detection of aqueous samples by drying has been eliminated. Hence, the sensitivity in detection can be improved substantially. To demonstrate the performance of the new substrates for biological samples, nucleobases of adenine, cytosine, thymine, and uracil were used.

## EXPERIMENTAL SECTION

**Materials and Reagents.** Silver nitrate was purchased from J.T. Baker (Phillipsburg, NJ). Methanol was obtained from Echo Chemical (Toufen, Taiwan). Poly(vinylidene difluoride) (PVDF) pellets and *p*-aminothiophenol (pATP) were obtained from Aldrich (Milwaukee, WI). Ammonium hydroxide (28–30%, w/v) was obtained from Acros Organics (Phillipsburg, NJ). Adenine, cytosine, and thymine were purchased from Alfa Aesar (Ward Hill, MA). Uracil and D-( $\beta$ )-glucose (anhydrous) were purchased from Sigma (St. Louis, MO). Sodium hydroxide (NaOH) was purchased from Yakuri Co. (Kyoto, Japan). DMF (*N,N*-dimethylformamide) was purchased from TEDIA (Fairfield, OH). All the chemicals were reagent grade, and deionized Milli-Q water was used to prepare all the aqueous solutions. PMMA optical fibers with different diameters were purchased from Hong-Yi Optical Fiber (Taichung, Taiwan).

**Instrumentation.** SERS spectra of probe molecules on POF substrates were collected using a Triax 320 Raman system (Jobin-Yvon, Inc., Longjumeau, France), equipped with a 35-mW, 632.8-nm He/Ne laser (JDS Uniphase Corporation, Milpitas, CA) and a liquid-nitrogen-cooled Ge CCD array detector (Jobin-Yvon, Inc.) at a resolution of 0.06 nm. The spectral acquisition time was 0.2 s for detection of pATP and 1 s for nucleobases unless specified. Scanning electron micro-

scope (SEM) investigations were performed using a JSM-7600F (JEOL, Ltd., Tokyo, Japan) FE-SEM operated at 3.0 kV.

**Preparation of Cylindrical SERS Substrates.** Several factors influence the preparation of the cylindrical SERS substrates. Cylindrical SERS substrates are named for this discussion as  $P^aA^bG^c t^d$ , where  $P^a$  represents dip coating in  $a$  % (w/v) PVDF solution,  $A^b$  represents the reaction in  $b$  mM AgNO<sub>3</sub> solution,  $G^c$  represents reduction in  $c$  M glucose, and  $t^d$  represents  $d$  min silver mirror reaction time. All of the PMMA substrates were cleaned by sonicating in methanol for 1 min before use. The substrates were dip-coated with PVDF dissolved in DMF at concentration  $a$ % (w/v) and dried vertically in a fume hood for 10 min with the tips pointed up. The PVDF solution was prepared by dissolving PVDF pellets in DMF using stirring overnight at room temperature. Tollens' reagent was prepared by mixing 50  $\mu$ L of 1 M NaOH with 5 mL of  $b$  mM silver nitrate in an ice bath to form a dark-brown solution. Ammonium hydroxide solution was added to this mixture drop by drop. The amount of ammonium hydroxide was controlled to have a final concentration of 6 times the concentration of silver nitrate. Similar to the setup in our previous study,<sup>17</sup> PMMA fibers were hung vertically in the reaction solution by a styrene-foam holder. After placement of the holder over the reaction solution for 5 min, 1.5 mL of glucose at a concentration of  $c$  M was added to the solution with careful stirring to ensure complete mixing. The beaker was removed from the ice bath and placed into a 55 °C water bath to react for  $d$  min. The silver-coated substrates were removed from the reaction solution and rinsed with deionized water before air drying. For initial characterization, the silver-coated substrates were immersed in 10  $\mu$ g/mL methanolic solution of pATP for 30 min. After the substrates were rinsed twice with methanol, SERS spectra were acquired. For detection of nucleobases, solutions were deposited on the tip of the substrates and spectra acquired immediately without drying. In this study, PMMA fiber with 2-mm diameter was mainly used because it provides better performance than other diameter fibers (see Supporting Information, Figure S1).

## RESULTS AND DISCUSSION

### Basic Properties of Novel Cylindrical SERS Substrates.

To characterize the new SERS substrates, pATP was used to probe the surfaces. Typical SERS spectra of pATP chemically adsorbed on  $P^{15}A^{20}G^{0.5}t^{20}$  and a planar substrate of AgNPs@ glass prepared by the method in our previous study<sup>17</sup> are shown in Figure 2. The solvent-subtracted spectra of 4% (w/v) pATP detected by conventional Raman scattering spectroscopy are also shown in Figure 2. Both substrates clearly show the expected bands, including as  $\nu$ (C–S) at 1088  $\text{cm}^{-1}$ ,  $\delta$ (C–H) at 1179  $\text{cm}^{-1}$ , and  $\nu$ (C=C) at 1594  $\text{cm}^{-1}$ .<sup>40,41</sup> The SERS spectrum shows prominent bands at 1575, 1434, 1387, 1140, and 1070  $\text{cm}^{-1}$ , which are inconspicuous in conventional Raman spectra. With the exception of bands located at 1589 and 1084  $\text{cm}^{-1}$ , the observed bands have similar positions both in bulk and in solution. The SERS spectra observed using the new substrates all were similar in spectral features and relative intensities between bands. Therefore, the intense band located at 1434  $\text{cm}^{-1}$  was chosen for use as an indication for optimization of the preparation procedures.

**Effect of DMF in the Preparation of Cylindrical SERS Substrates.** PVDF was used to roughen the tip of PMMA fibers and to increase the hydrophobicity of the tips for holding aqueous sample drops. However, the hydrophobic nature of

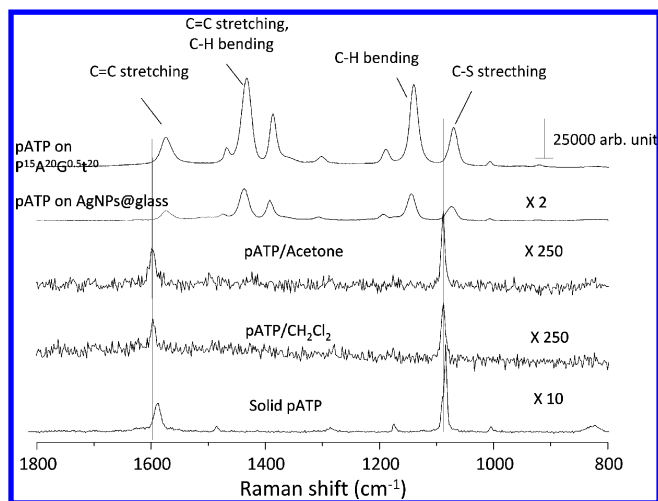


**Figure 2.** Typical SERS spectra of pATP on cylindrical substrates prepared in this work and on AgNPs@glass substrate. Raman spectra of 4% (w/v) pATP dissolved in acetone and dichloromethane and solid pATP also are shown for comparison.

PVDF limits the ability to attract AgNPs produced by the silver mirror reaction. To overcome this drawback, DMF was selected to dissolve PVDF for coating and to assist the adsorption of AgNPs. DMF has been used as reducing agent to form AgNP and AuNP colloids in the past.<sup>42–44</sup> To study the influence of DMF on the preparation of cylindrical SERS substrates, 2 mm diameter PMMA fibers were used. After dip-coating in 10% (w/v) PVDF/DMF solution, these fibers were suspended in air for different lengths of time to evaporate the DMF to different degrees. After exposure to the silver mirror reaction, the  $P^{10}A^{50}G^{0.5}t^4$  substrates were probed with pATP. The observed SERS intensities were plotted against drying time as shown in Figure 3. This figure shows that the SERS intensities remained similar for the first 15 min of drying time but started to decrease as the drying time of DMF was extended. This may indicate either that DMF assists the reduction of AgNPs at the SERS substrates or that evaporation of DMF causes differences

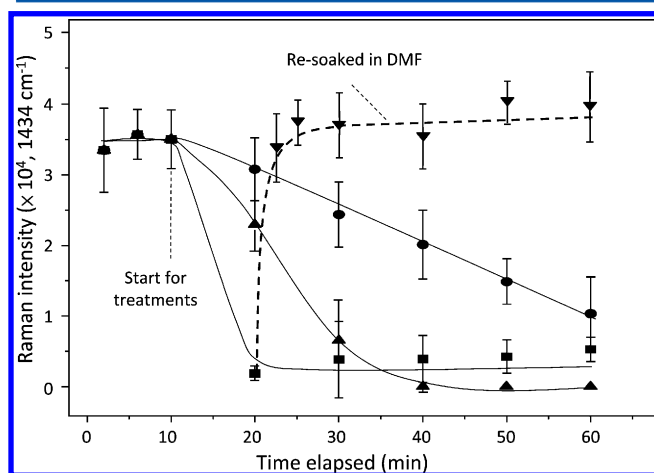


**Figure 3.** SERS intensities of pATP on  $P^{10}A^{50}G^{0.5}t^4$  substrates. These substrates were pretreated by air-drying for different times (▲), or air-drying for 10 min and then soaked in water (●) and methanol (■) for different times before the silver mirror reaction. To revive the substrates, they were re-soaked in 50% DMF (in water) for different times after soaking in methanol for 10 min (▼).

in compactness or roughness of the PVDF layer that influence the SERS intensities. To clarify, freshly coated substrates were air-dried for 10 min and then immediately soaked in water or methanol to remove the residual DMF. This treatment limited the disturbances to the compactness of the PVDF coatings. After these treatments, the silver mirror reaction was used to prepare  $P^{10}A^{50}G^{0.5}t^4$  substrates. The resulting SERS intensities are plotted in Figure 3, which shows that the substrates soaked in methanol and water have behavior similar to that of air-dried substrates. However, the rate of decrease in the SERS intensities is much faster than air drying. These results clearly indicate that DMF assists in formation of AgNPs.

To further ascertain the role of DMF, PVDF-coated substrates were air-dried for 10 min followed by cleaning in methanol for another 10 min. Following air-drying for 10 min, these substrates were re-soaked in water containing 50% (v/v) of DMF for different lengths of time. After re-soaking, the silver mirror reaction was performed in the same way as for freshly prepared substrates. The observed SERS intensities of these substrates are also plotted in Figure 3 against the re-soaking time in DMF solution. The plot clearly shows that re-soaking in DMF causes the observed SERS intensities to increase rapidly, similar to that for freshly prepared substrates. Also, the response curves indicated that the re-soaking time is not important, as the DMF can access the PVDF layer quickly. These results indicate that DMF assists the reduction/adsorption of AgNPs in formation of SERS substrates. To simplify the preparation, PVDF was dissolved in DMF for tip-coating and the substrates were air-dried for only 10 min.

**Optimization of Parameters for Preparation of Cylindrical SERS Substrates.** To optimize the conditions for preparation of cylindrical SERS substrates, several parameters were studied by systematic variation. These include the concentration of PVDF in the coating, the reaction time in silver mirror solutions, and the concentrations of silver nitrate and glucose in the silver mirror reaction. The effect of concentration of PVDF was first examined by preparation of substrates designated  $P^aA^{20}G^{0.5}t^{20}$ , where  $a$  was varied from 5 to 15. The SERS intensities obtained by probing with pATP are plotted in Figure 4A. A linear relationship between concentration of PVDF and the SERS signal was obtained, with the signal reaching a maximum around 12% (w/v). The higher concentrations of PVDF can form a thicker PVDF film on the PMMA tip and roughen the surface for holding a larger amount of AgNPs. Also, the thicker layer of PVDF retains the DMF more effectively, which increases the efficiency in reduction/adsorption of AgNPs. The solubility of PVDF in DMF is limited to ca. 20%; therefore, 15% PVDF solution is preferred for handling and treating the surface of PMMA.

To optimize the conditions in the silver mirror reaction, fibers coated in 15% PVDF solutions were used and the concentration of silver nitrate was varied. The results are plotted in Figure 4B, which shows that the reaction profiles were similar at different silver nitrate concentrations, and loading could be completed with 10 min of reaction time. When the concentration of silver nitrate reached 50 mM, a maximal SERS intensity was found around 4 min of reaction time. The decrease of SERS intensities for longer reaction times may result from formation of large particles having smaller SERS intensities. With the reaction time fixed at 20 min, the concentration of silver nitrate was varied, and the resulting SERS intensities for these substrates are plotted in Figure 4C. This plot shows that the largest SERS signal is obtained with a



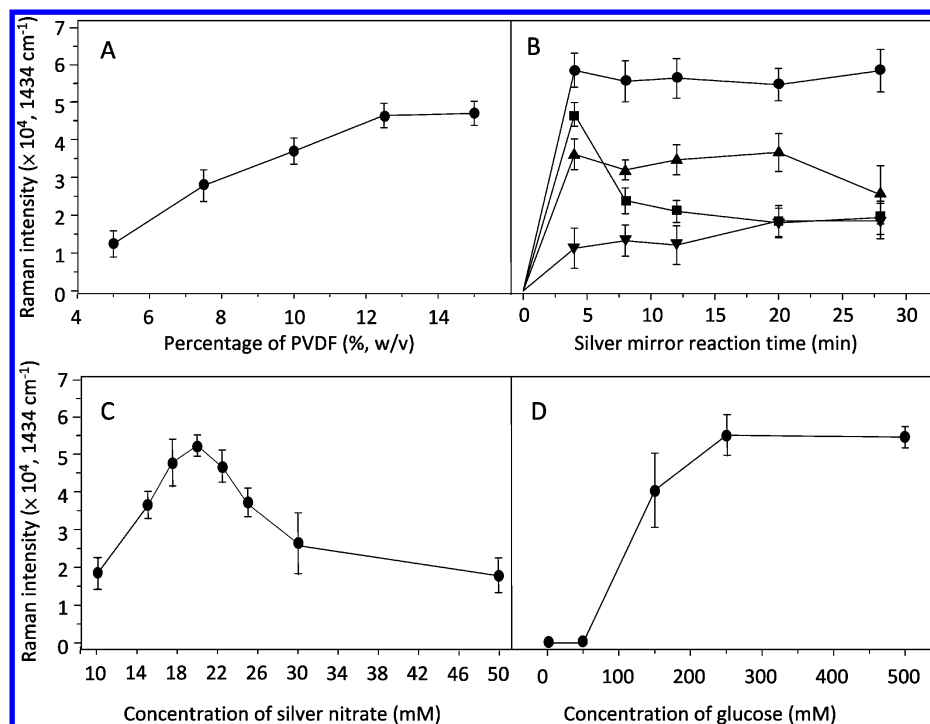


**Figure 4.** (A) SERS intensities for pATP on substrates  $P^aA^{50}G^{0.5}t^4$ , where  $a$  was varied from 0 to 15% (w/v). (B) Reaction time profiles for substrates of  $P^{15}A^bG^{0.5}t^d$ , where  $b$  was varied from 10 ( $\nabla$ ), 20 ( $\bullet$ ), 30 ( $\blacktriangle$ ), to 50 ( $\blacksquare$ ) and  $d$  was varied from 0 to 30. (C) SERS intensities for pATP on substrates of  $P^{15}A^bG^{0.5}t^{20}$ , where  $b$  was varied from 10 to 50. (D) SERS intensities for pATP on substrates of  $P^{15}A^{20}G^c t^{20}$ , where  $c$  was varied from 0 to 0.5.

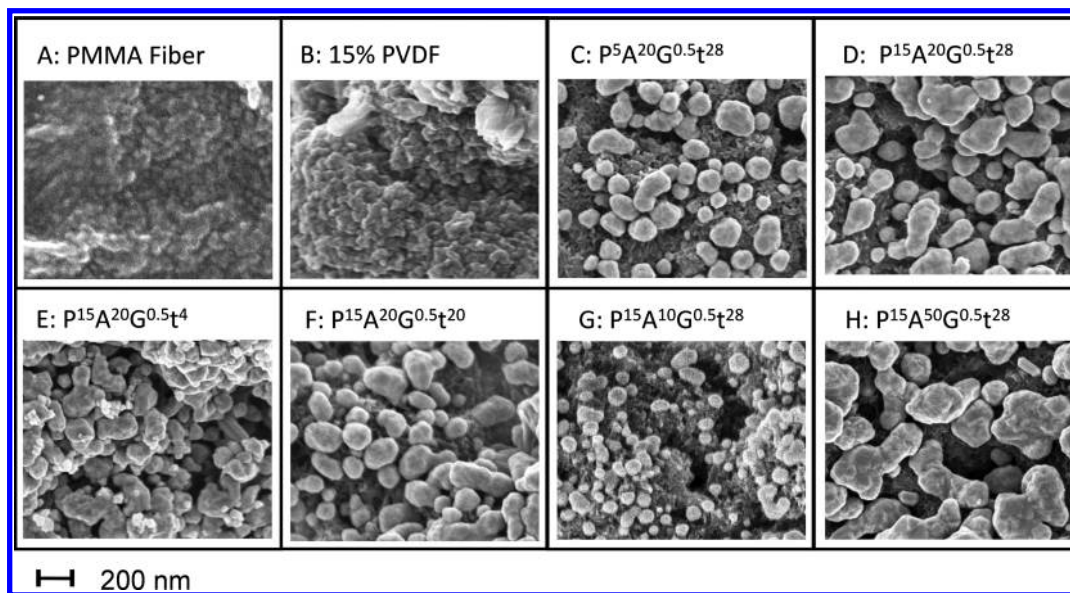


**Figure 5.** SEM images of the substrates (A) bare PMMA fiber, (B) 15% PVDF-coated fiber, (C)  $P^5A^{20}G^{0.5}t^{28}$ , (D)  $P^{15}A^{20}G^{0.5}t^{28}$ , (E)  $P^{15}A^{20}G^{0.5}t^4$ , (F)  $P^{15}A^{20}G^{0.5}t^{20}$ , (G)  $P^{15}A^{10}G^{0.5}t^{28}$ , and (H)  $P^{15}A^{50}G^{0.5}t^{28}$ .

silver nitrate concentration around 20 mM. Because DMF assists the formation of AgNPs, the effect of glucose concentration was examined by fixing the concentration of silver nitrate at 20 mM but varying the concentration of glucose from 50 mM to 0.5 M. The resulting SERS intensities for the corresponding substrates are plotted in Figure 4D. The results indicate that the glucose concentration should be kept higher than 250 mM to form with higher SERS intensities.

To explore the morphologies of AgNPs, substrates were scanned by SEM, and typical images are plotted in Figure 5.

The images in Figure 5A and 5B for the cross section of bare PMMA fiber and 15% PVDF-coated fiber clearly show that PVDF can increase the roughness of the fiber surface. To examine the influence of concentration of PVDF during coating, the substrates  $P^5A^{20}G^{0.5}t^{28}$  and  $P^{15}A^{20}G^{0.5}t^{28}$  were scanned, and the resulting images are shown in Figure 5C and 5D, respectively. The AgNPs were much larger in size for 15% PVDF coatings. As discussed above, this may be caused by better retention of DMF by thicker PVDF coatings. Again, it suggests that DMF affects the reduction and deposition of

AgNPs significantly. On the basis of Figures 5D to 5F, reaction time affects the size of the AgNPs. Longer reaction times produce larger AgNPs. Figure 5D represents the optimized preparation conditions, which include 15% PVDF with 20 mM AgNO<sub>3</sub> and 0.5 M glucose for 20 min silver mirror reaction time. When a higher concentration of silver nitrate was used, the reaction rate was significantly increased and the resulting AgNPs were larger in size for the same reaction time, as can be observed by comparing the images in Figure 5D, 5G, and 5H.

**Microanalysis of Aqueous Analytes Using Cylindrical SERS Substrates.** In recent years, SERS has been used in the biophysical and biochemical fields for rapid detection, quantification, and characterization of DNA and RNA segments.<sup>45–47</sup> It is a label-free technique and highly suited for direct detection of DNA bases as reported by several groups using colloidal Ag nanostructures for SERS detections.<sup>48–51</sup> To demonstrate that our SERS substrates can be used to detect nucleobases without drying, nucleobases including adenine, cytosine, thymine, and uracil in aqueous solution were examined. Cylindrical substrate arrays formed by substrates of P<sup>15</sup>A<sup>20</sup>G<sup>0.5</sup>t<sup>20</sup> were used. For quantitation of these samples, the sample volume was 4 μL and the integration time was 1 s. Typical SERS spectra of these nucleobases are shown in Figure 6, along with conventional Raman spectra of the solid

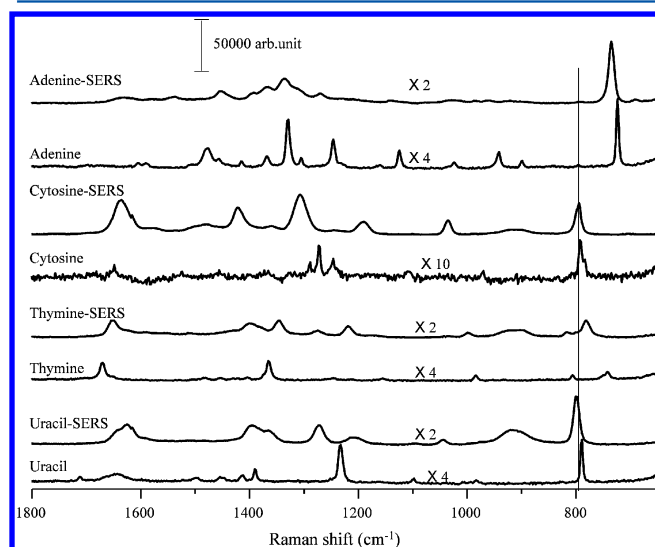


**Figure 6.** Conventional Raman spectra of adenine, cytosine, thymine, and uracil in solid form and their corresponding SERS spectra for nucleobases at concentrations of 100 μM. The sample volume was 4 μL, and the integration time for obtaining spectra was 1 s for these measurements.

nucleobases. All of the characteristic bands of nucleobases are clearly observed. The Raman intensities of these nucleobases are in the order of cytosine > adenine > uracil > thymine. This order indicates that AgNPs interact with cytosine more effectively. According to a previous study of AgNP–nucleobase interaction by a surface plasmon resonance band in the visible spectral region,<sup>52</sup> exocyclic nitrogen in cytosine takes part in binding AgNPs. Cytosine generates a lesser amount of canonical structures than other bases, allowing the AgNPs to strongly interact with it. Hence, the SERS intensities are stronger and generate well-defined bands.

To investigate the linear range of the SERS intensities for detection of nucleobases, different concentrations of adenine,

cytosine, thymine, and uracil were examined. One example for the relationship between SERS intensity at 735 cm<sup>-1</sup> and the concentration of adenine is plotted in Figure 7. This plot shows

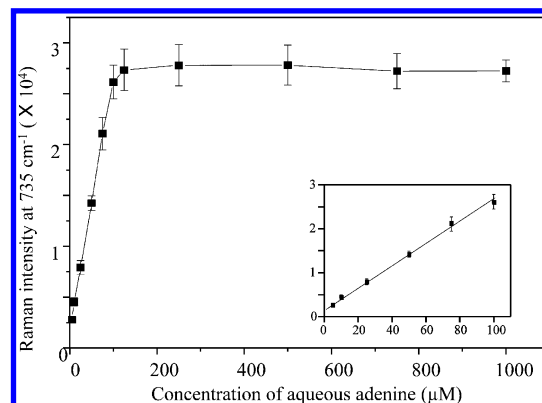


**Figure 7.** The concentration profile of adenine detected using a novel cylindrical SERS substrate. Four microliter sample droplets of various concentrations were detected using P<sup>15</sup>A<sup>50</sup>G<sup>0.5</sup>t<sup>20</sup> substrates. The inset shows the enlarged figure in the low concentration region.

that the SERS signal increases rapidly with the concentration of adenine and then approaches a maximum value at concentrations higher than 100 μM. This observation is similar for the other bases cytosine, thymine, and uracil, as shown in Table 1

**Table 1. Regression Coefficient, Detection Limit, and SERS Intensity for Ring Breathing Band around 800 cm<sup>-1</sup> for 5 μM Adenine, Cytosine, Thymine, and Uracil Using a 4 μL Sample with P<sup>15</sup>A<sup>50</sup>G<sup>0.5</sup>t<sup>20</sup> Substrates**

nucleobase	band (cm <sup>-1</sup> )	SERS inten (arbr unit) <sup>a</sup>	regression coefficient <sup>b</sup>	limit of detection (nM) <sup>c</sup>
adenine	735	2783 (±225)	0.998	215
cytosine	796	1778 (±225)	0.996	337
thymine	781	822 (±81)	0.995	730
uracil	798	1561 (±53)	0.994	384

<sup>a</sup>SERS intensities for 5 μM nucleobase. <sup>b</sup>Concentration ranges from 2.5 to 100 μM. <sup>c</sup>Based on S/N = 3.

(also see Supporting Information, Figures S2 to S4). The linear regression coefficients in the different concentration ranges were calculated. The results show that the regression coefficient ( $R^2$ ) is higher than 0.99 for concentrations lower than 100 μM. To estimate detection limits for nucleobases using the new cylindrical substrates, nucleobases at a concentration of 2.5 μM were examined. Based on a detection limit criterion of 3 times the noise level in the blank test, the estimated detection limit is 215 nM when the intensity of the ring breathing band at 735 cm<sup>-1</sup> is used. To evaluate the magnitude of enhancement factor (EF) in detection of adenine, the following equation has been used.

$$EF = (I_{\text{SERS}}/I_{\text{Raman}}) \times (N_{\text{bulk}}/N_{\text{ads}})$$

where  $I_{\text{SERS}}$  is the SERS intensity of particular peak of probe molecule while  $I_{\text{Raman}}$  is the intensity for the same band in the Raman spectrum in liquid form.  $N_{\text{ads}}$  is the number of adenine molecules in the 4 μL drop of aqueous solution, and  $N_{\text{bulk}}$  is the number of adenine molecules in 1% (w/v) aqueous solution exposed to the laser. The estimated enhancement factor was approximately  $1.21 \pm 0.09 \times 10^7$  for the SERS detection of

adenine under the optimized conditions described. Because the aqueous sample on SERS substrate was not dried, only the molecules of adenine close to the surface of AgNPs can be enhanced. Therefore, the calculated enhancement factor was underestimated.

## CONCLUSIONS

In this work, we have prepared a new type of low-cost versatile cylindrical SERS substrate array and demonstrated its use to study the nucleobases in aqueous systems. It is important to note that a simple approach has been employed for the preparation of silver nanoparticles on an inert membrane of PVDF formed by solvent deposition. Microliter volumes of nucleobase solutions have been loaded with high reproducibility and detected within a few minutes without disturbing the system with heat or organic solvents. The results shown here indicate that cylindrical substrates with a microdroplet of analyte on the tip are a promising approach to application of SERS for mass analysis of trace-level biologically important species in aqueous systems.

## ASSOCIATED CONTENT

### Supporting Information

Additional information as noted in the text. This material is available free of charge via the Internet at <http://pubs.acs.org>.

## AUTHOR INFORMATION

### Corresponding Author

\*Tel: +886-422840411 ext. 514. Fax: +886-422862547. E-mail: [jiyis@dragon.nchu.edu.tw](mailto:jiyis@dragon.nchu.edu.tw).

### Notes

The authors declare no competing financial interest.

## ACKNOWLEDGMENTS

The authors thank the National Science Council of Republic of China for financial support for this work.

## REFERENCES

- (1) Yoon, I.; Kang, T.; Choi, W.; Kim, J.; Yoo, Y.; Joo, S. W.; Park, Q. H.; Ihee, H.; Kim, B. *J. Am. Chem. Soc.* **2009**, *131*, 758–762.
- (2) Campion, A.; Kambhampati, P. *Chem. Soc. Rev.* **1998**, *27*, 241–250.
- (3) Zhou, Q.; Li, X.; Fan, Q.; Zhang, X.; Zheng, J. *Angew. Chem., Int. Ed.* **2006**, *45*, 3970–3973.
- (4) Moskovits, M. *J. Raman Spectrosc.* **2005**, *36*, 485–496.
- (5) Genov, D. A.; Sarychev, A. K.; Shalae, V. M.; Wei, A. *Nano Lett.* **2004**, *4*, 153–158.
- (6) Brolo, A. G.; Germain, P.; Hager, G. J. *J. Phys. Chem. B* **2002**, *106*, 5982–5987.
- (7) Yang, X. M.; Tryk, D. A.; Hashimoto, K.; Fujishima, A. *J. Phys. Chem. B* **1998**, *102*, 4933–4943.
- (8) Lee, P. C.; Meisel, D. *J. Phys. Chem.* **1982**, *86*, 3391–3395.
- (9) Leopold, N.; Lendl, B. *J. Phys. Chem. B* **2003**, *107*, 5723–5727.
- (10) Chaney, S. B.; S. Shanmukh, S.; Dluhy, R. A.; Zhao, Y. P. *Appl. Phys. Lett.* **2005**, *87*, 031908.
- (11) Bao, L.; Mahurin, S. M.; Haire, R. G.; Dai, S. *Anal. Chem.* **2003**, *75*, 6614–6620.
- (12) Farquharson, S.; Shende, C.; Inscore, F. E.; Maksymiuk, P.; Gift, A. *J. Raman Spectrosc.* **2005**, *36*, 208–212.
- (13) Lee, Y. H.; Dai, S.; Young, J. P. *J. Raman Spectrosc.* **1997**, *28*, 635–639.
- (14) Ni, F.; Cotton, T. M. *Anal. Chem.* **1986**, *58*, 3159–3163.
- (15) Saito, Y.; Wang, J. J.; Batchelder, D. N.; Smith, D. A. *Langmuir* **2002**, *18*, 2959–2961.
- (16) Park, H. K.; Yoon, J. K.; Kim, K. *Langmuir* **2006**, *22*, 1626–1629.
- (17) Cheng, M. L.; Yang, J. *Appl. Spectrosc.* **2008**, *62*, 1384–1394.
- (18) Qu, L.; Dai, L. *J. Phys. Chem. B* **2005**, *109*, 13985–13990.
- (19) He, Y.; Wu, X.; Lu, G.; Shi, G. *Nanotechnology* **2005**, *16*, 791–796.
- (20) Tran, C. D. *Anal. Chem.* **1984**, *56*, 824–826.
- (21) Laserna, J. J.; Campiglia, A. D.; Winefordner, J. D. *Anal. Chim. Acta* **1988**, *208*, 21–30.
- (22) Ota, F.; Higuchi, S.; Gohshi, Y.; Furuya, K.; Ban, M.; Kyoto, M. *J. Raman Spectrosc.* **1997**, *28*, 849–854.
- (23) Niu, Z.; Fang, Y. *J. Colloid Interface Sci.* **2006**, *303*, 224–228.
- (24) Cao, Y. W. C.; Jin, R.; Mirkin, C. A. *Science* **2002**, *297*, 1536–1540.
- (25) Ruan, C.; Wang, W.; Gu, B. *Anal. Chem.* **2006**, *78*, 3379–3384.
- (26) Braun, G.; Lee, S. J.; Dante, M.; Nguyen, T. Q.; Moskovits, M.; Reich, N. *J. Am. Chem. Soc.* **2007**, *129*, 6378–6379.
- (27) Zavaleta, C.; de la Zerda, A.; Liu, Z.; Keren, S.; Cheng, Z.; Schipper, M.; Chen, X.; Dai, H.; Gambhir, S. S. *Nano Lett.* **2008**, *8*, 2800–2805.
- (28) Vo-Dinh, T.; Hiromoto, M. Y. K.; Begun, G. M.; Moody, R. L. *Anal. Chem.* **1984**, *56*, 1667–1670.
- (29) Kneipp, J.; Kneipp, H.; Kneipp, K. *Chem. Soc. Rev.* **2008**, *37*, 1052–1060.
- (30) Nie, S.; Emory, S. R. *Science* **1997**, *275*, 1102–1106.
- (31) Kneipp, K.; Wang, Y.; Kneipp, H.; Perelman, L. T.; Itzkan, I.; Dasari, R. R.; Feld, M. S. *Phys. Rev. Lett.* **1997**, *78*, 1667–1670.
- (32) Hankus, M. E.; Cullum, B. M. *SPIE-Int. Soc. Opt. Eng., Proc.* **2007**, *6759*, 6759081–67590810.
- (33) Hankus, M. E.; Li, H.; Gibson, G. J.; Cullum, B. M. *Anal. Chem.* **2006**, *78*, 7535–7546.
- (34) Hankus, M. E.; Cullum, B. M. *SPIE-Int. Soc. Opt. Eng., Proc.* **2006**, *6380*, 23–34.
- (35) Hankus, M. E.; Gibson, G.; Chandrasekharan, N.; Cullum, B. M. *SPIE-Int. Soc. Opt. Eng., Proc.* **2004**, *5588*, 106–116.
- (36) Huang, G. G.; Han, X. X.; Hossain, M. K.; Osaki, Y. *Anal. Chem.* **2009**, *81*, 5881–5888.
- (37) Erol, M.; Han, Y.; Stanley, S. K.; Stafford, C. M.; Du, H.; Sukhishvili, S. *J. Am. Chem. Soc.* **2009**, *131*, 7480–7481.
- (38) Mijovic, J.; Luo, H. L.; Han, C. D. *Polym. Eng. Sci.* **1982**, *22* (4), 234–240.
- (39) Liu, F.; Hashim, N. A.; Liu, Y.; Abed, M. R. M.; Li, K. *J. Membr. Sci.* **2011**, *375*, 1–27.
- (40) Kim, K.; Yoon, J. K. *J. Phys. Chem. B* **2005**, *109*, 20731–20736.
- (41) Cao, L.; Diao, P.; Tong, L.; Zhu, T.; Liu, Z. *Chem. Phys. Chem.* **2005**, *6*, 913–918.
- (42) Pastoriza-Santos, I.; Liz-Marzán, L. M. *Nano Lett.* **2002**, *2*, 903–905.
- (43) Pastoriza-Santos, I.; Liz-Marzán, L. M. *Langmuir* **1999**, *15*, 948–951.
- (44) Kamat, P. V. *J. Phys. Chem. B* **2002**, *106*, 7729–7744.
- (45) Otto, C.; Tweel, T. J. J. v. d.; Mul, F. F. M. d.; Greve, J. *J. Raman Spectrosc.* **1986**, *17*, 289–298.
- (46) Liu, R.; Zhu, S.; Si, M.; Liu, Z.; Zhang, D. *J. Raman Spectrosc.* **2012**, *43*, 370–379.
- (47) Badr, Y.; Mahmoud, M. A. *Spectrochim. Acta, Part A* **2006**, *63*, 639–645.
- (48) Kneipp, K.; Kneipp, H.; Kartha, V. B.; Manoharan, R.; Deinum, G.; Itzkan, I.; Dasari, R. R.; Feld, M. S. *Phys. Rev. E* **1998**, *57*, R6281–R6284.
- (49) Lin, H.; Mock, J.; Smith, D.; Gao, T.; Sailor, M. J. *J. Phys. Chem. B* **2004**, *108*, 11654–11659.
- (50) Chan, S.; Kwon, S.; Koo, T.-W.; Lee, L. P.; Berlin, A. A. *Adv. Mater.* **2003**, *15*, 1595–1598.
- (51) Maruyama, Y.; Ishikawa, M.; Futamata, M. *Chem. Lett.* **2001**, *8*, 834–835.
- (52) Basu, Y.; Jana, S.; Pande, S.; Pal, T. *J. Colloid Interface Sci.* **2008**, *321*, 288–293.